X-711-68-91

PREPRINT

NASA TM X- 63175

A SPACECRAFT ANALOG-TO-DIGITAL CONVERSION SYSTEM EMPLOYING MOSFETS

DONALD C. LOKERSON

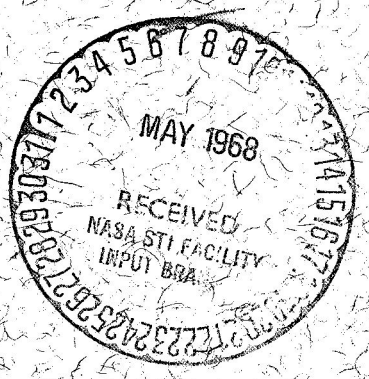

MARCH 1968

GSFC

GODDARD SPACE FLIGHT CENTER

GREENBELT, MARYLAND

ABSTRACT

The analog-to-digital conversion system described includes an analog commutator, 5 millisecond gated voltage-to-frequency converter, and storage of the digital output to 0.5% resolution of a 0 to +5 volts input. Because of its ultra-high input impedances and compactness, the system components could be useful in a broad scope of applications.

CONTENTS

ILLUSTRATIONS

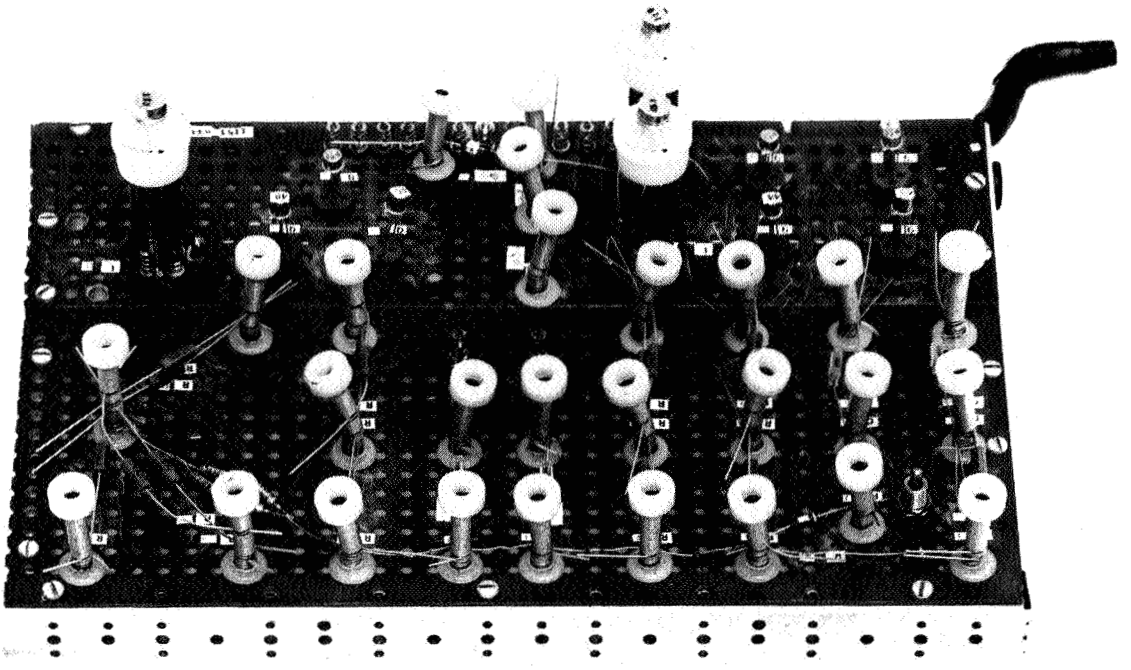

Frontispiece—The analog oscillator in three stages of assembly.

A SPACECRAFT ANALOG-TO-DIGITAL CONVERSION SYSTEM EMPLOYING MOSFETS

by
Donald C. Lokerson
Goddard Space Flight Center

INTRODUCTION

The Interplanetary Monitoring Platform (IMP) Spacecrafts contain sensors which produce voltages proportional to temperature, current, and other parameters, which must be commutated into an analog-to-digital converter. This conversion is performed by gating the output of a voltage-controlled-oscillator into a binary accumulator for a fixed time period. Because this conversion averages the sensor voltage over the sample period, greater immunity to noise can be achieved than with the more conventional successive approximation analog-to-digital converter.

Recent advances in the production of Metal-Oxide-Semiconductor-Field-Effect-Transistors (MOSFETS) have allowed the analog system to take advantage of the excellent properties of the devices. They have extremely high-input-impedance gates and are easily integrated on one chip in large quantities. The analog commutator, voltage-controlled oscillator, and accumulator are mainly composed of integrated circuit MOSFETS.

The system to be described in detail commutates analog voltages from ground to plus five volts into a linear voltage-to-frequency oscillator which can be gated "on" for 5.0 milliseconds. The output frequency of 6 kilocycles to 46 kilocycles is accumulated by an 8 bit binary counter which is completely integrated on one chip.

A history of similar systems employed in the past and areas explored during this development will provide a comparison of systems which have been considered. Then a detailed discussion of the system to be used in future IMP spacecrafts will serve as one example of the possible applications of MOSFETS in analog-to-digital conversion.

HISTORY OF THE DEVELOPMENT OF THIS ANALOG-TO-DIGITAL CONVERTER

Previous IMP spacecraft employed Pulse Frequency Modulation (PFM) channel coding of both analog and digital data. Voltage-controlled oscillators were employed to produce these pulse frequencies directly from the analog voltages. A 5 kilocycle to 15 kilocycle magnetic-core multivibrator was selected because of the long term stability. On IMP D&E, an 8 bit accumulator was used to digitize some of the analog data by sampling the oscillator frequency for 20 milliseconds.

Future spacecraft will require A to D conversions as frequently as every 5 milliseconds, thus a new oscillator will be required. The difficulties in temperature compensation of the magnetic-core oscillator and the desire to cover a much wider frequency range made other methods of controlling the oscillator frequency attractive. The IMP D&E oscillator required presetting an accumulator and allowing it to overflow once before the normal readout occurred. Thus it could "underflow" if the frequency became too low. With the new design, avoiding such a possibility was desirable.

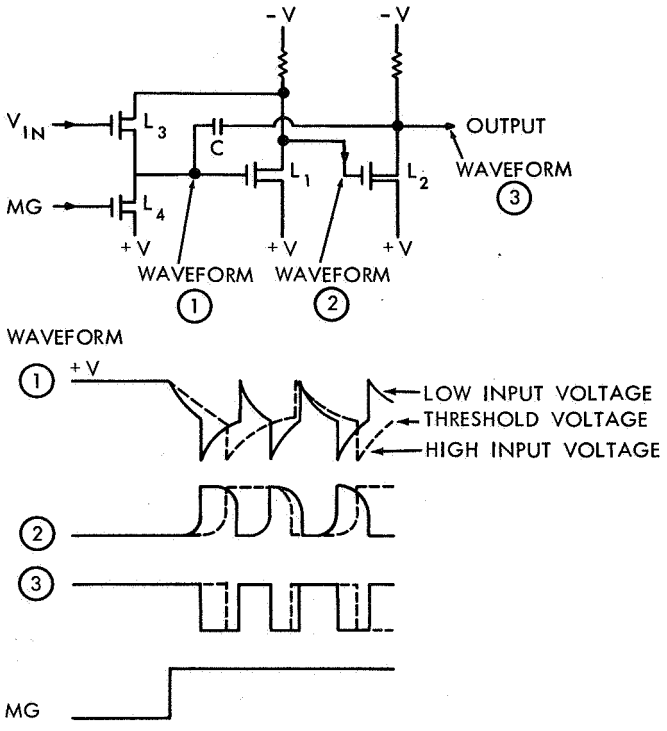

Figure 1—Second MOSFET oscillator considered.

The first analog oscillator studied employed a constant current discharge of a variable height sawtooth; however, short term stability and linearity were poor due to difficulty in controlling the sawtooth resetting.

The second approach employed the MOSFET circuit in Figure 1. As V_{IN} is made more negative, the effective impedance of L_3 decreases, thus increasing the oscillator frequency. The MOSFET changed impedance too quickly to operate over the 5 volt range desired, thus further development was not considered.

The third MOSFET analog oscillator proved most promising because linearity and temperature coefficients could be compensated well, over a very wide range of frequency. This will be described in detail.

A class of linear-period oscillators was discounted because the distortion in transfer function is detrimental, as shown in Figure 2. The digitization accuracy is not constant across the voltage range, which is also undesirable. Figure 2 transforms a temperature sensor voltage response through three transformations, yielding the A/D output versus temperature.

SYSTEM REQUIREMENTS

The design goals for the IMP H, I, & J spacecraft analog-to-digital conversion are:

1. Normal input voltage range = 0 to +5 volts
2. Operating input voltage range = -0.5 to +5.5 volts
3. Digitization resolution = 0.5%
4. Calibration and linearity over normal voltage range
   a. +10°C to +30°C = ±1/2 count
   b. -5°C to +45°C = ±1 count

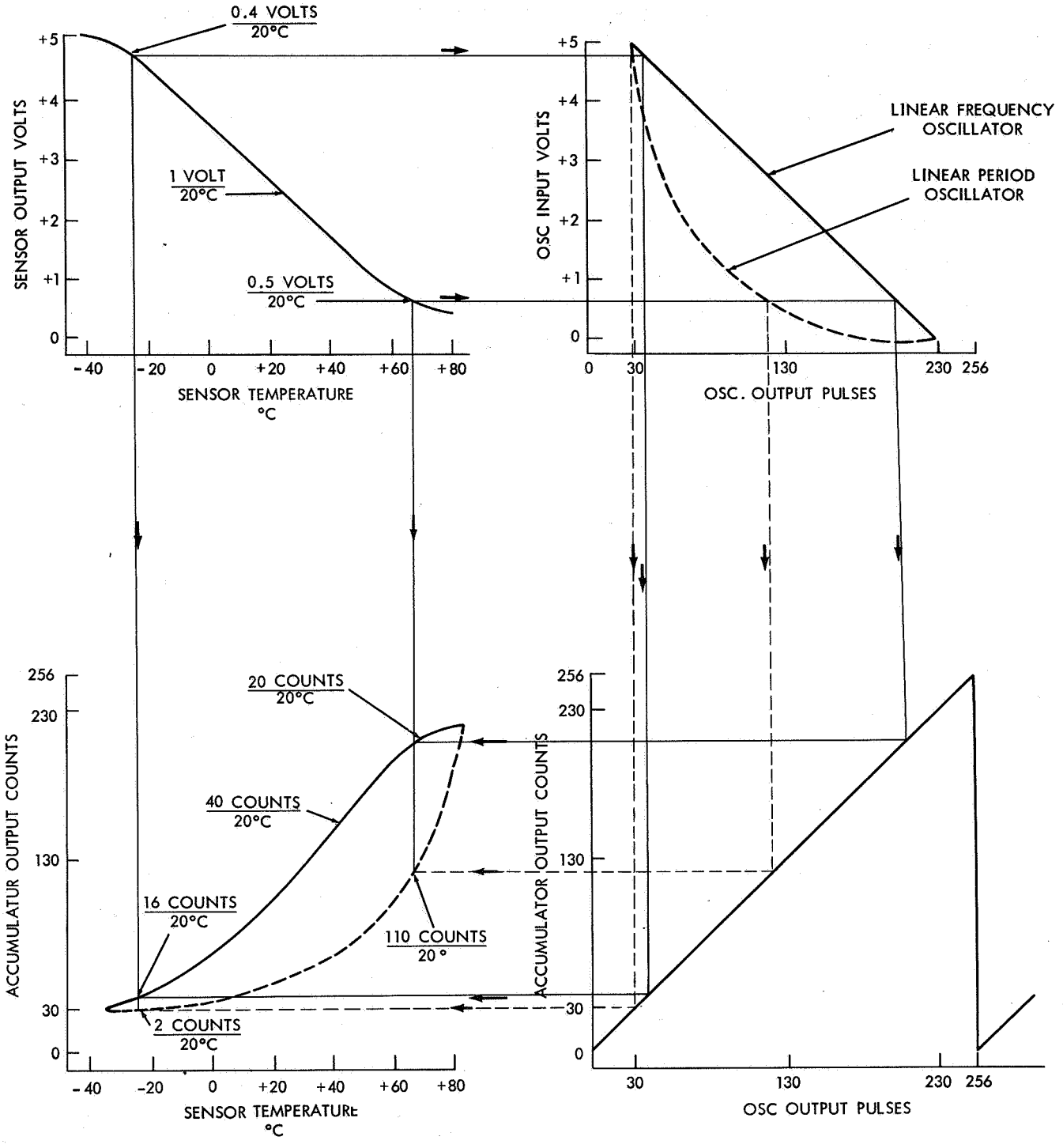

Figure 2—Effect of oscillator linearity.

c. -35°C to +85°C = ±3 counts

5. Voltage input loading by analog oscillator:

   a. less than .04 microamperes at ground

   b. more than 5 megohms at 5 volts

6. Ground-to-five volt square wave input voltage response to be within ±2 counts of 2.5 volt input calibration
7. First day after turn-on stability = ±2 counts
8. Short term stability = ±1/2 count
9. Long term stability = ±2 counts
10. Consistency between oscillators over the -5° to +45°C range = ±1 count
11. Analog sample period = 2.5 Ms or 5.0 Ms.

An 8 bit accumulator has a digital output range of 256 counts, or slightly better than 0.5% resolution. The oscillator nominal voltage input range of 0 to +5 volts requires an output range of 200 counts, but a "safety margin" of 0.5 volts would be desirable. The 56 extra counts should be divided nearly equally above and below the nominal extremes, thus defining the frequency of the oscillator as:

$$\frac{\text{5 volts range}}{\text{200 counts range}} = 25 \frac{\text{millivolts}}{\text{count}} \text{ resolution}$$

A similar calculation for a 5 millisecond sample time yields a 6 to 46 kilocycle range for the oscillator.

The oscillator should operate nearly linearly over a large range, from 5.5 volts to -0.5 volts, so that:

$$\frac{\text{30 counts at 5 volts}}{2.5 \times 10^{-3} \text{ seconds per sample}} = \text{12 kilocycles at 5 volts}$$

$$\frac{\text{230 counts at 0 volts}}{2.5 \times 10^{-3} \text{ seconds per sample}} = \text{92 kilocycles at 0 volts}$$

where:

$$\frac{\text{10 counts at 5.5 volts}}{2.5 \times 10^{-3} \text{ seconds per sample}} = \text{4 kilocycles at +5.5 volts}$$

$$\frac{\text{250 counts at -0.5 volts}}{2.5 \times 10^{-3} \text{ seconds per sample}} = \text{100 kilocycles at -0.5 volts}$$

A similar calculation for a 5 millisecond sample time yields a 2 to 50 kilocycle range for the oscillator. This voltage-controlled oscillator must operate approximately linearly over nearly 5 octaves!

The input commutator may have up to 50 inputs commutated into the one analog oscillator. The oscillator output may be gated into several binary counters for data storage until readout by the spacecraft telemetry.

THE MOSFET DEVICE

A detailed description of the METAL OXIDE SEMICONDUCTOR FIELD EFFECT TRANSISTOR (MOSFET) is necessary because of their particular properties, and because many similar devices are produced by industry. The "P" channel MOSFET is constructed on an N type "body" with two P-doped diffusions, as shown in Figure 3. A layer of silicon dioxide insulates an aluminum "gate" from the device. As the gate is made more negative than the more positive P region, a channel is formed, as shown in Figure 3, producing characteristics as shown in Figure 4, when used as an inverter. The MOSFET is used as a saturated inverter switch in the analog commutator and in the digital circuits in the accumulator.

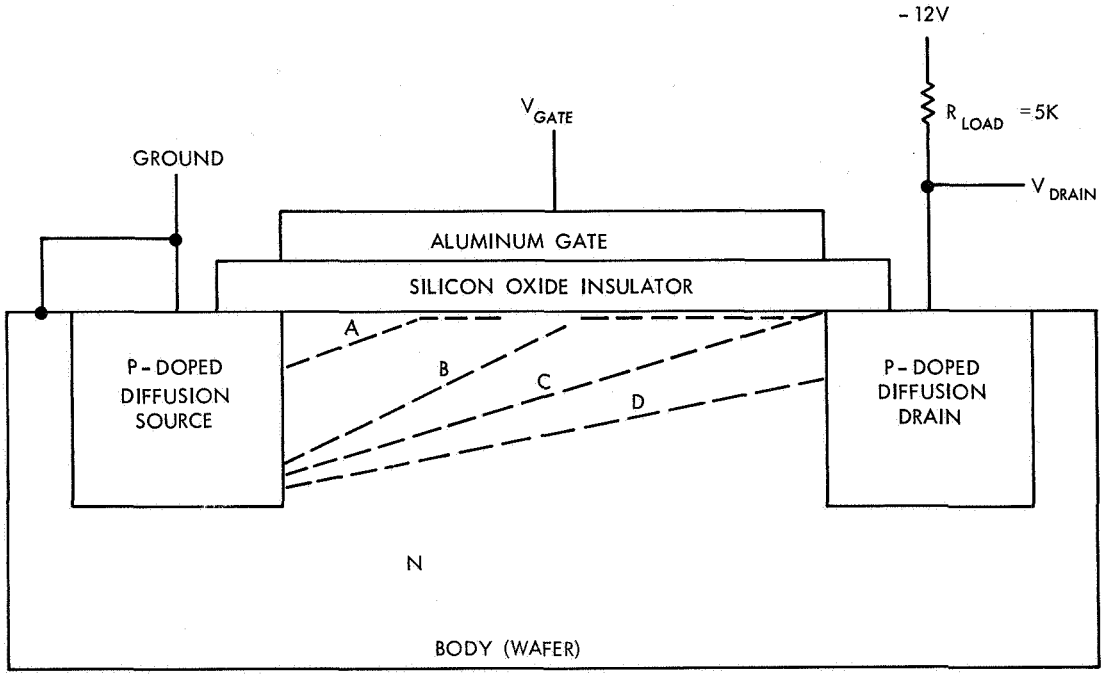

LOGICIAL STATE	GATE VOLTAGE	DRAIN VOLTAGE	APPROXIMATE VOLTAGE-AMPERAGE CHARACTERISTIC	CHANNEL LABEL
HARD OFF	- 3 VOLTS	- 12 VOLTS	CURRENT LIMITED	A
ALMOST OFF	- 4 VOLTS	- 11 VOLTS	CURRENT LIMITED	B
PARTY ON	- 7 VOLTS	- 2 VOLTS	OHMIC	C
HARD ON	- 12 VOLTS	- 1 VOLT	OHMIC	D

(ASSUME 4 VOLT THRESHOLD DEVICE)

Figure 3—The MOSFET as an inverter.

Part of the analog oscillator utilizes the MOSFET as an emitter follower, or source follower. Figure 5 shows the change in gate-to-source voltage as a function of current through the device. In general any linear change in the oscillator with voltage input can be calibrated out, but any non-linearity is difficult to cancel out. The non-linear change in this device is about 10% over the entire range of interest (10 to 250 microamps), but is less than 1% if the two piece-wise approximations can be made. As explained later, the analog oscillator will achieve this result by employing two different source followers, both determining the frequency when less than +3 volts is put into the oscillator. Only one source follower determines the frequency when more than about +3 volts is put into the oscillator. Slightly different

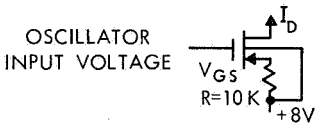

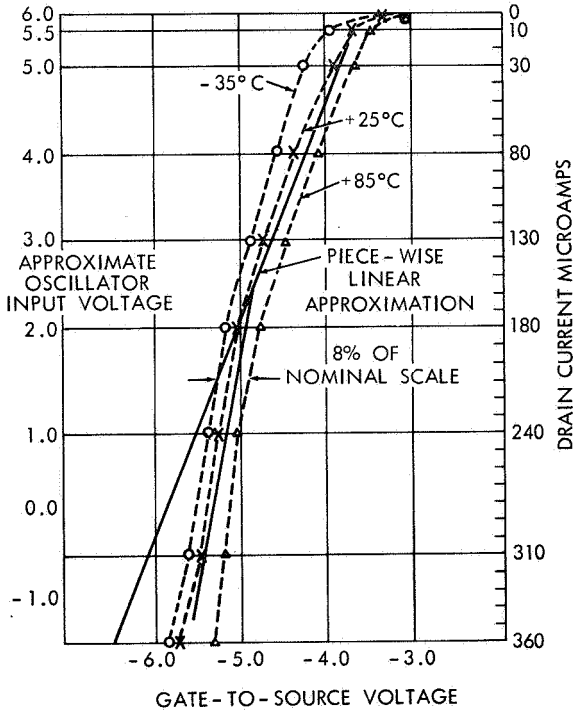

Figure 5—Source follower MOSFET characteristic.

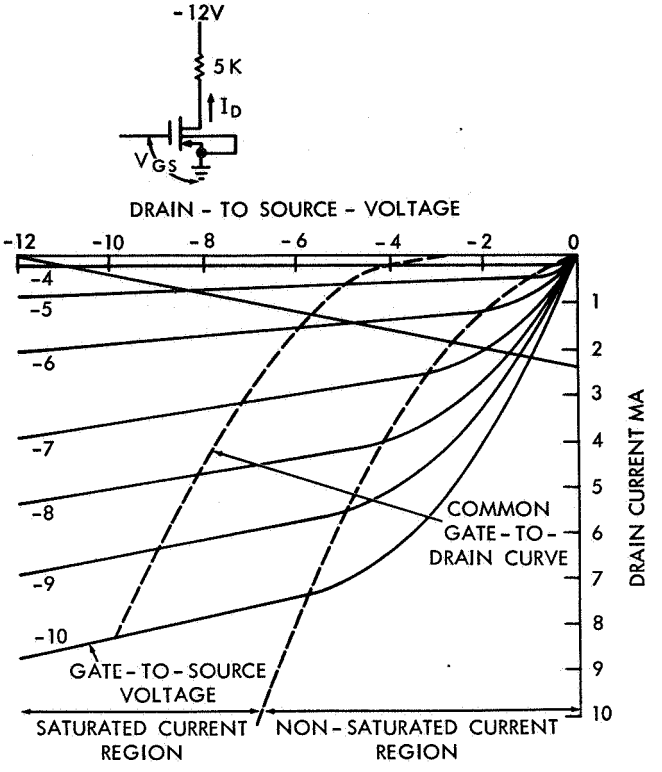

Figure 4—Inverter MOSFET drain characteristic at room temperature.

values for R in the two source followers will produce a nearly linear result.

The temperature effects on the MOSFET when used in the source follower circuit are quite large, but nearly linear, as shown in Figure 5. The 0.15 volt decrease in gate-to-source voltage from -35°C to 25°C is about equal to the 0.15 volt decrease from 25°C to 85°C. This drop in voltage will be compensated by a corresponding voltage drop in the +8 volt regulator supply as the temperature increases. When the gate and drain are maintained at nearly equal voltages, the MOSFET gate-to-source voltage varies linearly with temperature, as shown in Figure 6. This properly will be utilized in the MOSFET regulator as described later.

The MOSFETS used in the analog oscillator almost completely determine the oscillator's voltage-to-frequency characteristics, and it is

only because of the particular voltage-to-current characteristics of these devices that the analog oscillator described later can be made linear and temperature-compensated to a high degree.

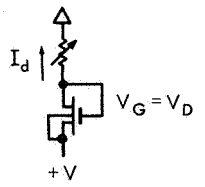

THE ANALOG COMMUTATOR

The IMP spacecraft encoding systems will include an analog data processor, which multiplexes voltage monitors, temperature monitors, and experiment sensor outputs into one analog-to-digital converter, as shown in Figure 7. PP1, PP2, and PP3 are shown in this simplified example. The resistors R_{IN} are 100 kilohms to 500 kilohms, and represent a constant load impedance to the experiment, with the remainder of the commutator appearing as an insignificant additional load. The resistor R_{LIMIT} is about 1 kilohm to limit the current drawn if a very high positive voltage is put into the terminal PP1. Diode D_1 clamps the voltage so that L_1 will be able to turn off by application of +8 volts to the gate of L_1. This prevents cross-talk to other sensors being commutated. The body lead of L_1 must be more positive than the +8.7 volts to which the source is clamped, to prevent leakage. When commutation of PP1 into the analog-to-digital converter is desired, square waves A, B, and C are all negative, turning that branch of the logic matrix "on." The positive voltage on the gate of L_4 turns device L_4 "off." The -10 volts applied to L_1 gate is sufficient to turn the L_1 device hard "on" even if the input PP1 is at ground. The L_1 device is about 1 kilohm impedance when the gate is more than 6 volts more negative than the source. The L_1 device is hundreds of megohms when the gate is +8 volts.

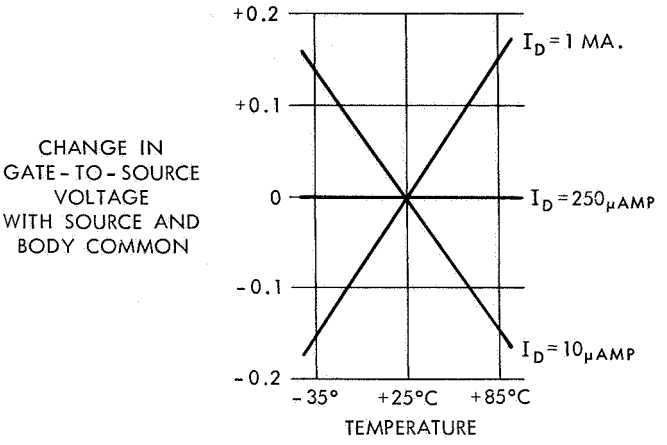

Figure 6—Ideal variation in gate-to-source voltage with temperature.

As the waveforms in the logic matrix change, several microseconds are required for the new analog voltage to be gated "on," due to the high resistor values which conserve power. The analog-to-digital converter will not begin taking a sample until at least 2.5 milliseconds after the new analog data line switching has begun. Thus this circuit conserves power by allowing non-critical switching times. Negligible additional loading (hundreds of megohms) of the sensor develops during the commutation of the analog voltage.

THE ANALOG OSCILLATOR

The MOSFET source follower characteristics produce a 4% non-linearity current output due to the non-linear change in gate-to-source voltage with current. The current as shown in Figure 8 will determine the frequency of a multivibrator, producing approximately the same non-linearity

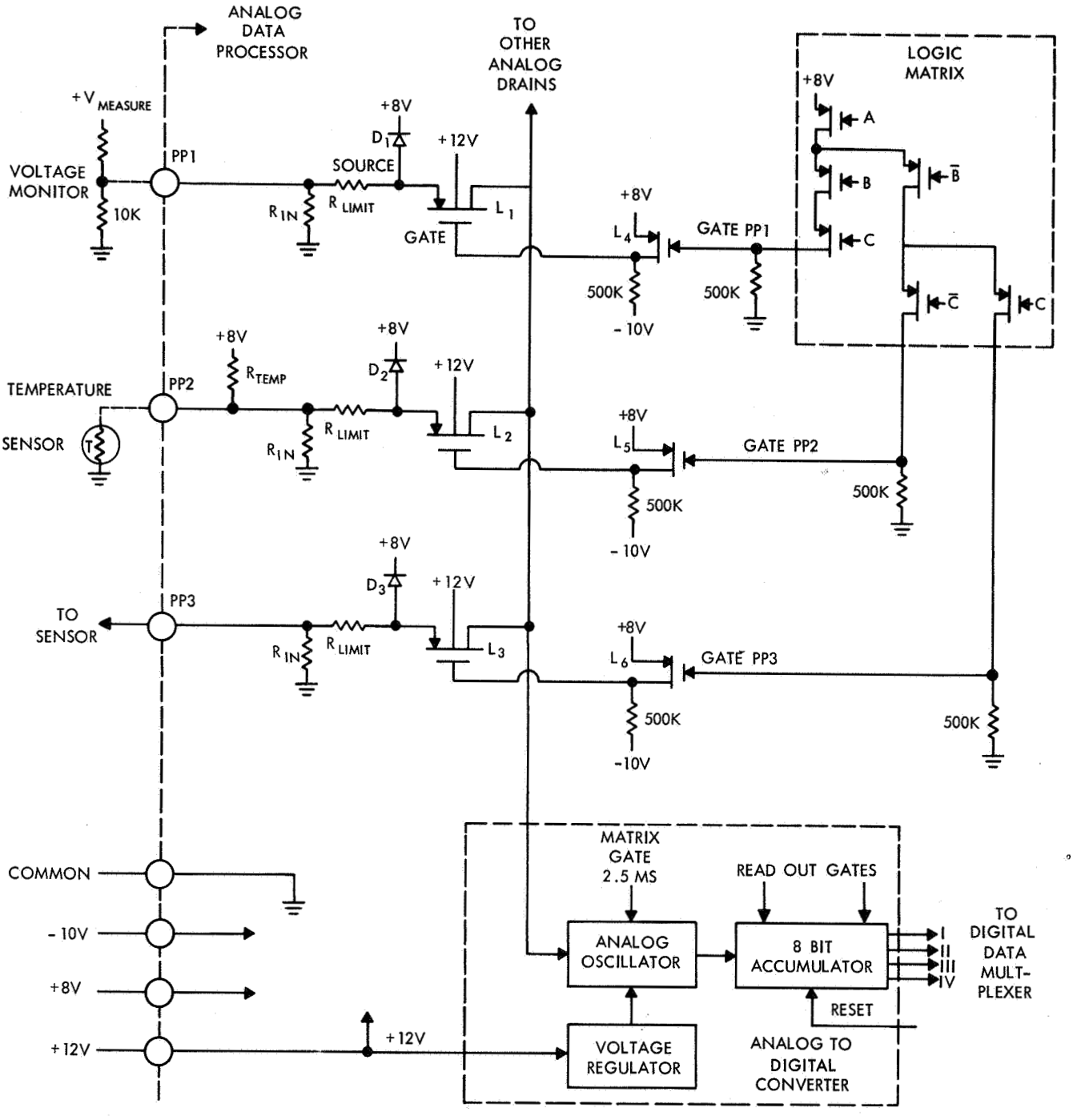

Figure 7—Simplified analog data processing system.

in frequency. The operation of the multivibrator begins with Q_1 "off" and Q_2 "on." The current I_1 will charge C_1 in some time period τ_1 until Q_1 is turned "on." This forces the base of Q_2 to go negative almost +V volts. This turns Q_2 "off," causing the base of Q_1 to go even more positive, thus reinforcing the switching action. Then I_2 charges C_2 during a time period τ_2, until Q_2 is turned "on" again, thus turning Q_1 "off." This switching action returns the oscillator to the original state. Since the input voltage-to-current characteristic is non-linear, then a similar non-linearity

will occur in the voltage-to-frequency characteristic, producing a higher than desired frequency at high currents, as shown in Figure 9. However, if R_1 is made infinite, and R_3 provides a nearly constant current to C_1, the output frequency will approach $1/\tau_1$ as I_2 increases and τ_2 approaches zero. Note that this is the opposite effect from when I_1 supplied current; thus a combination of I_1, I_2, and I_3 can be selected to approach a linear characteristic. This is shown mathematically as approximately:

$$\frac{i_n}{C_n} = \frac{dV_{saw\ tooth}}{dt}$$

or

$$\int_0^{\tau_n} dt = \int_{V_{sw_n}}^{+0.5V} \frac{C_n}{I_n}\, dv$$

$$T_n = \frac{C_n}{I_n}\left(V_{sw_n} + 0.5\right)$$

$$f_{OUT} = \frac{1}{\tau_1 + \tau_2 + \tau_{SWITCHING}} = \frac{1}{\frac{C_1(V_{sw}+0.5)}{I_1+I_3} + \frac{C_2(V_{sw}+0.5)}{I_2}}$$

where in practice:

$$|V_{sw_n} + 0.5| \approx |V|$$

$$C_1 \approx C_2 \approx C$$

$$V_1 \approx V_2 \approx V_{IN} + V_{GS}$$

$$T_{SWITCHING} \rightarrow 0$$

$$I_1 = \frac{V - V_{IN} - V_{GS}}{R_1}$$

$$I_2 = \frac{V - V_{IN} - V_{GS}}{R_2}$$

$$I_3 \approx \frac{3V}{2R_3} \text{ (averaged)}$$

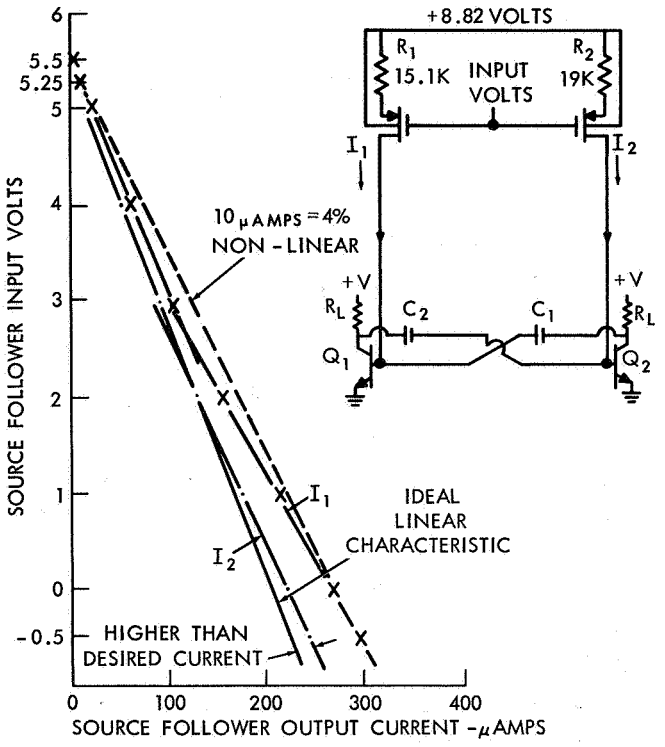

Figure 8—MOSFET source follower input to analog oscillator.

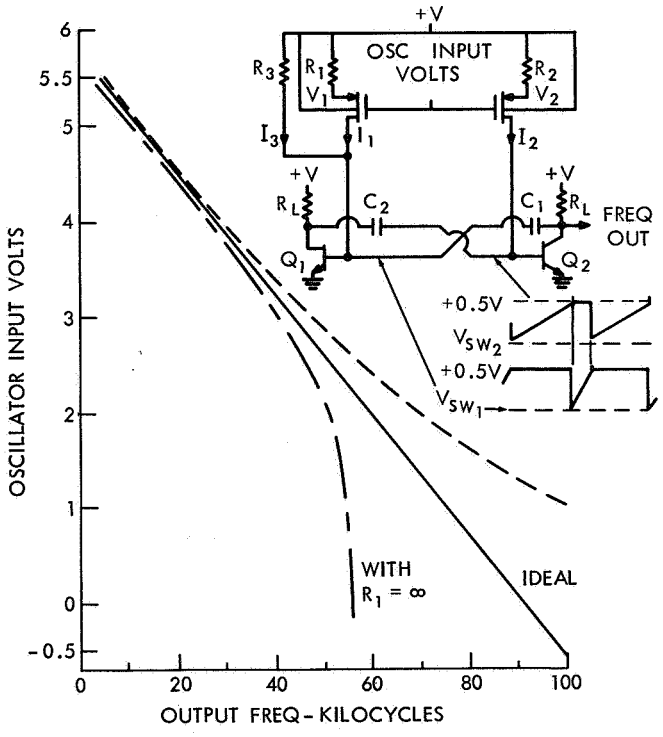

Figure 9—Linearity correction characteristic.

$$f_{OUT} \approx \frac{1}{V\left(\frac{C}{I_1 + I_3} + \frac{C}{I_2}\right)} = \frac{1}{CV\left(\frac{1}{I_1 + I_3} + \frac{1}{I_2}\right)} = \frac{V - V_{IN} - V_{GS}}{CV\left(\frac{1}{\frac{1}{R_1} + \underbrace{\frac{3V}{2R_3(V - V_{IN} - V_{GS})}}_{\text{LINEARITY CORRECTION TERM}}} + R_2\right)}$$

if I_3 is negligible, then:

$$f_{OUT} \approx \frac{1}{CV\left(\frac{1}{I_1} + \frac{1}{I_2}\right)} = \frac{1}{CV\left(\frac{R_1 + R_2}{V - V_{IN} - V_{GS}}\right)} = \frac{V - V_{IN} - V_{GS}}{CV(R_1 + R_2)}$$

Thus, the non-linear input MOSFETS voltage-to-current characteristic is cancelled by the non-linear effect to the multivibrator of the linearity correction term I_3.

As the input voltage, V_{IN}, increases, the frequency output decreases. Any change in threshold voltage, V_{GS}, produces the same amount of change in frequency as an equal change in the input voltage V_{IN} would produce. The same change in the supply voltage, V, will change the output frequency only about 2/3 as much because the sawtooth amplitude changes to help compensate. Since V_{GS} will change due to temperature, radiation, and other effects, the supply voltage, V, will make a corresponding change, such that:

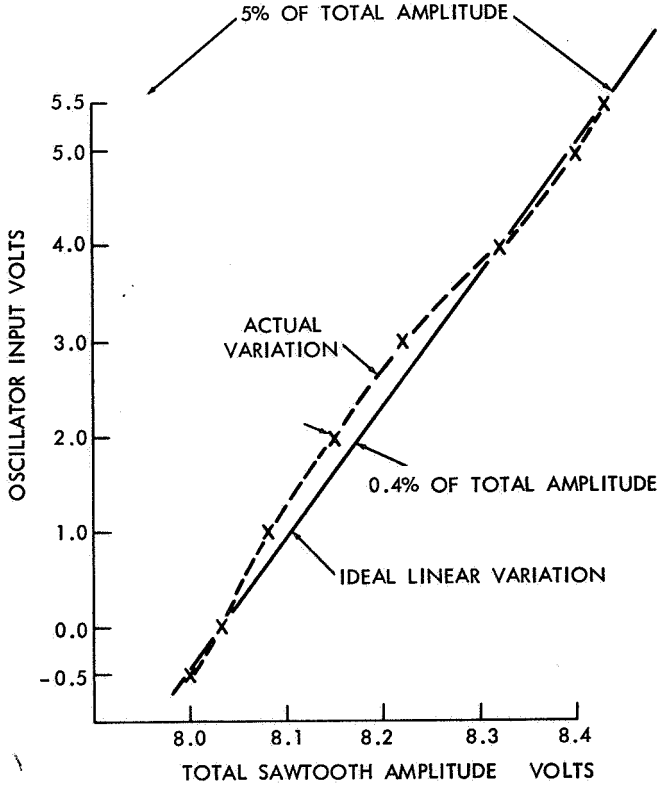

Figure 10—Multivibrator sawtooth variations.

$$f_{OUT} \approx \frac{(V + \Delta V_{GS}) - V_{IN} - (V_{GS} + \Delta V_{GS})}{K} \approx \frac{V - V_{IN} - V_{GS}}{K}$$

A MOSFET within the voltage regulator will perform this function.

The multivibrator is not a perfect current-to-frequency converter; thus some of these characteristics must be considered. As the currents I_1 and I_3 increase, the transistors Q_1 and Q_2 will be held on harder, increasing the storage time at the moment of switching. The total sawtooth voltage amplitude, $V_{s\omega}$, varies due to this effect, as shown in Figure 10. A small increase in the Q_1 and Q_2 base diode drops also occurs with increased current. The total sawtooth amplitude plotted in Figure 10 is nearly linear; thus this variation is calibrated out of the oscillator.

When low frequencies are generated at high input voltages, the current required to turn Q_1

or Q_2 "on" is dependent on the value of the load resistors R_L. Since the oscillator should still operate with less than 5 microamperes flowing into the Q_2 base at 5.5 volts, a complimentary multivibrator was substituted for the simpler version, as shown in Figure 11. The 0.1 microampere steady state base current into Q_7 and Q_8 is capacitively bypassed to provide very fast multivibrator switching at very low frequencies. If a voltage higher than +6.0 volts should exist for even a short instant, the multivibrator would stop operating, due to lack of current I_2. The ability to resume multivibrating when the signal drops again to within normal limits is doubtful, and it depends on the fall time of the signal when within the normal voltage range again. To prevent such a problem, a minimum multivibrator frequency is determined by resistor R_4, in Figure 11.

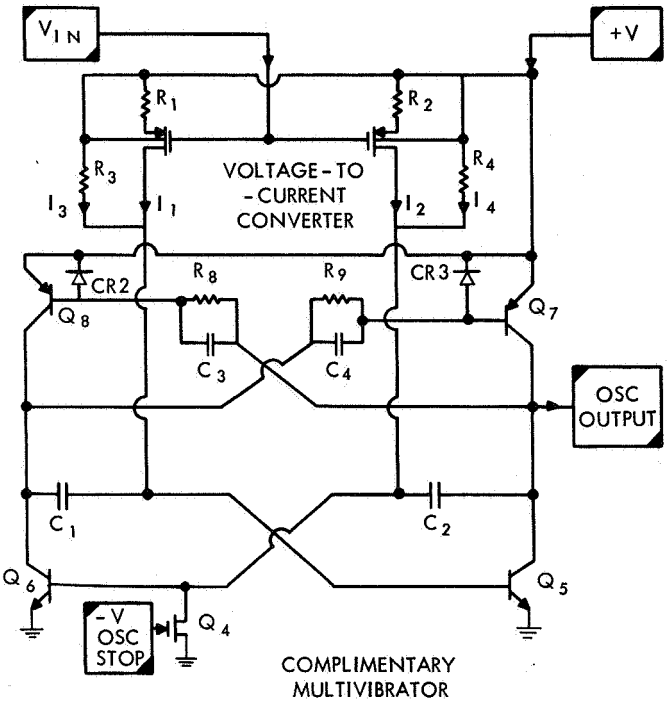

Figure 11—Complete oscillator circuit.

The operation of the entire oscillator can now be understood. The analog-to-digital conversion of the voltage V_{IN} is accomplished by gating the oscillator output frequency into an accumulator. To achieve the maximum resolution, of plus one count and minus no counts, the initial phase of the oscillator operation should be at the same point at the beginning of the sample. If MOSFET Q_4 in Figure 11 is held "on" for 2.5 milliseconds, then Q_6 will be held "off" while I_3 and I_1 will hold Q_5 "on." This will turn Q_8 "on" and Q_7 "off." At the time a sample is to begin, Q_4 is quickly turned "off" by pulling "-Vosc stop" above ground. Then current I_2 and I_4 will charge capacitor C_2 until Q_6 begins to turn "on." This will turn Q_7 "on" and Q_5 "off," thus reinforcing the Q_6 "turn-on" process, until the switching is complete, with Q_5 and Q_8 "off" and Q_7 and Q_6 "on." The base of Q_5 is now at -(+V) and slowly increases as C_1 is charged by I_1 and I_3, until Q_5 begins to turn "on" and the circuit returns to the original state, except that Q_6 base is then at -(+V). Oscillation continues at a frequency determined by I_1, I_2, I_3, and I_4 until stopped by a negative voltage at "-V osc stop."

The capacitors C_3 and C_4 are large enough to fully switch Q_8 and Q_7, with only R8 and R9 holding the circuit in the steady state. CR2 and CR3 clamp the turning off transient of Q_8 and Q_7 respectively, so that only 1 volt base change is required to turn the Q_8 or Q_7 "on."

The "-Vosc stop" voltage must be about -9 volts to turn Q_4 "on" well. If V_{IN} is a large negative voltage, I_2 becomes quite large, and the internal "on" resistance of Q_4 could allow Q_6 to turn "on" when not desired. Thus a limit to the negative voltage possible is desirable. The MOSFET commutator will prevent more than a -5 volt input of -V = 9 volts.

The characteristics of the multivibrator over a temperature range of -35°C to +85°C is mainly dependent on the timing capacitors C_1 and C_2, since the transistor gain changes do not affect the

saturated logic of the complimentary switch multivibrator significantly. Consequently C_1 and C_2 are very stable high quality capacitors. The linear temperature characteristic of these capacitors, as shown in Figure 12, have only a 0.1% non-linearity in capacitance change with temperature. The +140 parts per million per degree centigrade temperature coefficient will be calibrated out by the oscillator power regulator. The resistors employed in the voltage-to-current generator change less than 25 parts per million per degree centigrade from -55°C to +175°C. The 0.3% change in resistance is small enough to neglect over the normal operating temperature range.

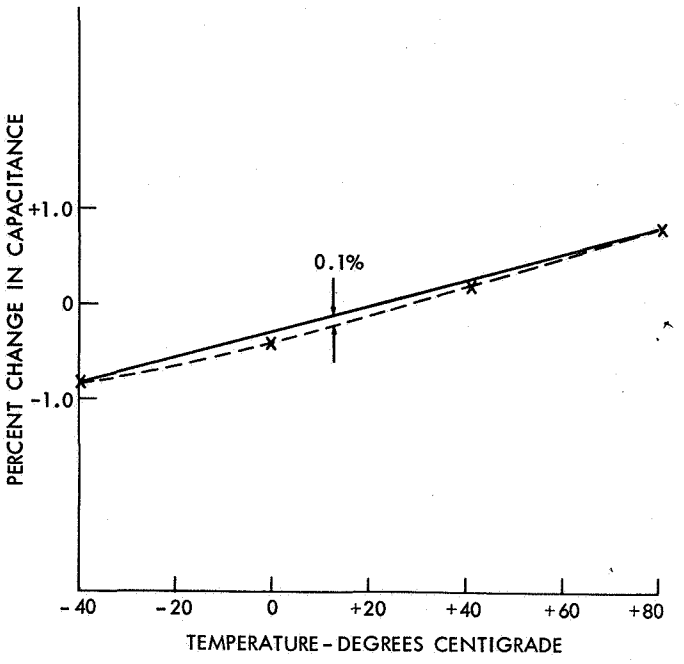

Figure 12—Capacitor temperature characteristic.

THE VOLTAGE REGULATOR

The analog oscillator frequency depends greatly on the supply voltage from which it is powered. This voltage is adjusted to determine the frequency at +5.0 volts, and must change with temperature to compensate for the temperature coefficients of the MOSFETS and capacitors. Any small change in threshold voltage in the input MOSFETS must be compensated for by the power regulator. Thus a voltage reference using a MOSFET was chosen, with the original circuit shown in Figure 13a. The input voltage "V_P" is around 12 volts, and the required regulated voltage is about 8 volts; thus Q_{11} drops the voltage difference of about 4 volts. The regulated voltage is divided by R5 and R6 to produce a voltage V_1. The MOSFET Q_3 acts like a poor Zener diode voltage source when its gate and drain are connected together as was shown in Figure 4; thus $V_2 = V_{REG} - V_{GS}$. The difference amplifier Q_9 and Q_{10} amplifies any difference between V_1 and V_2, and increase or decrease the current to correct the voltage difference. If the oscillator input voltage decreases, the current increases, and the regulated voltage decreases slightly by some ΔV. The original voltages are indicated as unprimed symbols and voltages after the change in current are primed nomenclature, in the equations below.

Assuming that Q_9 and Q_{10} loading can be neglected:

$$V_1 = V_{REG}\left(\frac{R_6}{R_5 + R_6}\right)$$

$$V_2 = V_{REG} - V_{MOS}$$

where V_{MOS} is the source-to-drain voltage

$$V_1' = (V_{REG} + \Delta V)\left(\frac{R_6}{R_5 + R_6}\right)$$

$$V_2' = (V_{REG} + \Delta V) - V_{MOS}'$$

$$\Delta(V_1 - V_2) \approx (V_1 - V_1') + (V_2 - V_2') = \left(\frac{R_6}{R_5 + R_6}\right)(V_{REG} - V_{REG} - \Delta V)$$

$$+ (V_{REG} - V_{MOS} - V_{REG} - \Delta V + V_{MOS}')$$

$$\approx \left(\frac{R_6}{R_5 + R_6}\right)(\Delta V) - \Delta V - V_{MOS} + V_{MOS}'$$

where $V_{MOS} \approx V_{MOS}'$ and where $R_5 \approx R_6$

$$\Delta(V_1 - V_2) \approx -\Delta V\left(1 - \frac{R_6}{R_5 + R_6}\right) \approx -\Delta V\left(\frac{1}{2}\right)$$

Thus in this circuit Q_3 is used as a Zener diode, without utilizing the amplification available in the device. The regulation was improved by using the circuit shown in Figure 13b. The same equations as above still apply, except:

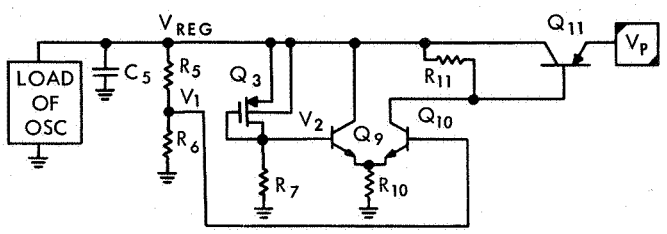

(a) ORIGINAL REGULATOR CIRCUIT

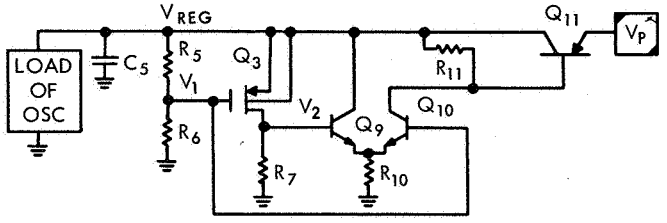

(b) IMPROVED REGULATOR CIRCUIT

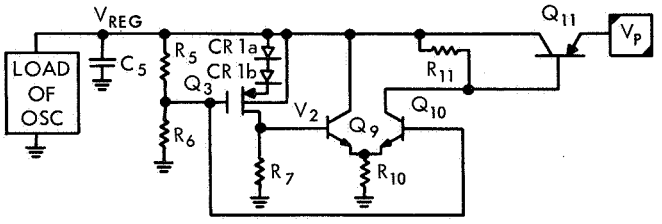

(c) FINAL REQULATOR CIRCUIT

Figure 13—Regulator circuits.

$$\Delta V_{gs} = \left[(V_{REG}' - V_1') - (V_{REG} \quad V_1)\right] = V_{REG}\left(1 - \frac{R_6}{R_6 + R_5}\right) + (V_{REG} + \Delta V)\left(1 - \frac{R_6}{R_6 + R_5}\right) = +\Delta V\left(1 - \frac{R_6}{R_6 + R_5}\right)$$

$$\Delta(V_1 - V_2) \approx \left(\frac{R_6}{R_5 + R_6}\right)(\Delta V) - \Delta V - V_{MOS} + V_{MOS}'$$

but now:

$$V_{MOS}' - V_{MOS} \approx \Delta V_{gs}\left(\frac{\partial V_d}{\partial V_{gs}}\bigg|_{I_d}\right) = \Delta V\left(1 - \frac{R_6}{R_6 + R_5}\right)(-\mu) = -\mu\left(1 - \frac{R_6}{R_6 + R_5}\right)\Delta V$$

where the amplification factor μ is typically about 40; therefore:

$$\Delta(V_1 - V_2) \approx -\left(1 - \frac{R_6}{R_5 + R_6}\right)\Delta V - \mu\left(1 - \frac{R_6}{R_6 + R_5}\right)\Delta V = \left(1 - \frac{R_6}{R_5 + R_6}\right)(\mu + 1)(-\Delta V)$$

$$\approx 20\,\Delta V \quad \text{if} \quad R_5 \approx R_6$$

Thus a small change in the regulator will produce a bigger change in the difference amplifier, resulting in about a 20 times larger closed loop gain in the improved circuit, as shown in Figure 13b. As the oscillator is cooled, the gain of Q_9, Q_{10} and Q_{11} decrease, but the gain of Q_3 increases, making the degree of regulation almost constant with temperature. As mentioned previously, the temperature coefficient of the MOSFET is linear and proportional to the current through the device if the gate and drain are connected together. This is still true in this improved circuit, because the difference amplifier holds V_1 very close to V_2. A comparison of the regulator outputs for these two circuits with a Zener diode is shown in Figure 14, in which direct substitution was made into the circuits shown in Figure 13.

The only problem which developed from the "improved" regulator circuit was that V_{MOS} voltage drop was only about half of the regulated voltage, at the current needed to achieve temperature compensation. Thus when a change in "threshold" voltage occurred in the devices in Q_1, Q_2 and Q_3, the regulator over-compensated by a factor of two. This can be shown mathematically as:

$$V_1 = V_{REG}\left(\frac{R_6}{R_5+R_6}\right) = V_{REG} - V_{MOS} = V_2$$

$$V_{REG} = + \frac{V_{MOS}}{\left(1 - \frac{R_6}{R_5+R_6}\right)}$$

where $R_6 \approx R_5$

$$V_{REG} \approx \frac{V_{MOS}}{1/2} = 2V_{MOS}$$

$$V'_{REG} \approx 2V_{MOS} + 2\Delta V_{MOS}$$

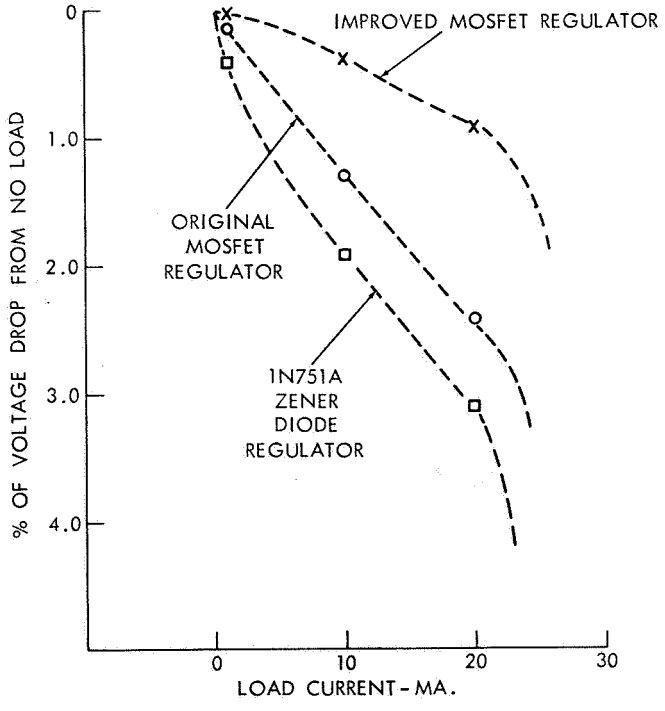

Figure 14—Comparison of regulator performance.

Thus the final regulator circuit, shown in Figure 13c, relieved this problem by three effects.

The placement of CR1 in the source lead makes the Q_3 MOSFET appear much more like the Q_1 and Q_2 MOSFETS in the oscillator near the +5 volts input because of the additional source-to-body voltage. The diodes CR1 also adds a large negative temperature coefficient to $V_{REG} - V_2$, which is cancelled out by a large increase in current through Q_3 which also increases its "threshold" voltage, as shown in Figure 15. The result was about a 2.5 volts larger voltage reference for the oscillator which makes

a change in "threshold" voltage of Q_1, Q_2 and Q_3 track more exactly. This is shown mathematically as:

$$V_1'' \approx V_{REG}(.2) \approx V_{REG} - V_{MOS}'' = V_2''$$

$$V_{REG} \approx \frac{V_{MOS}''}{.8} = \frac{5}{4} V_{MOS}''$$

$$V_{REG}' \approx \frac{5}{4} V_{MOS}'' + \frac{5}{4} \Delta V_{MOS}''$$

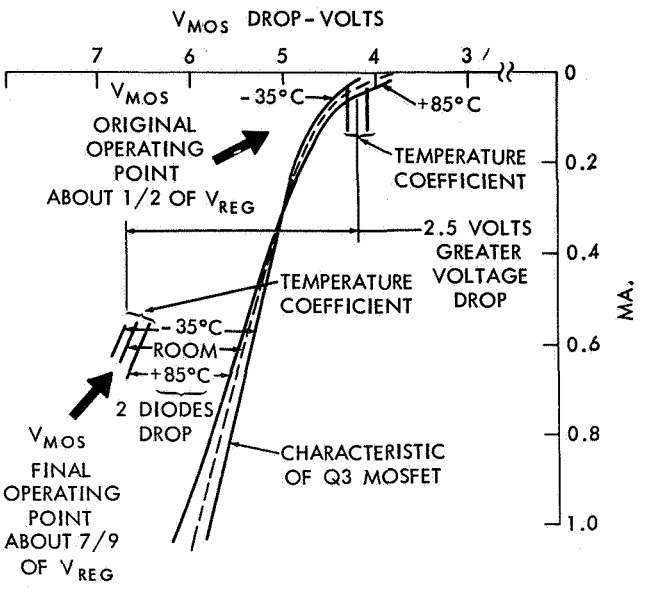

Figure 15—Change in voltage characteristics with additional CR1 diodes.

Thus a change in effective gate-to-source voltage on Q_1 and Q_2 MOSFETS due to temperature, radiation, or charge migration is compensated by about 5/4 as much change in the regulated supply. The addition of a third diode to increase V_{MOS}'' to almost equal V_{REG} becomes impractical unless dependence on a negative supply voltage is possible to operate the difference amplifier and supply current to Q_3. This well-regulated supply is not available in the system herein described; thus we will settle for this approximation.

This final regulator circuit is now able to regulate the voltage supplied to the analog oscillator, and varies almost the same as the MOSFETS within the oscillator as a function of temperature, radiation, and charge migration. The resistors R_5 and R_6 are used to set the +5 volt frequency of the oscillator at room temperature. The temperature coefficient of the oscillator is varied by changing R7. The maximum operating current is determined by R10, while the minimum current and ability to start with power turn-on is determined by R11. The transients and tendency to oscillate is reduced by C_5.

The circuit is extremely independent of the supply voltage V_P because Q_{11} supplies a current β times that sensed by the difference amplifier Q_9 and Q_{10}, nearly independent of the collector-to-emitter voltage. The voltage V_P must be at least 0.7 volts greater than the highest regulated supply requirements.

THE DIGITAL ACCUMULATOR

The output of the analog oscillator is accumulated in an eight bit binary counter. It is important to understand the sequence of events, so they are illustrated in Figure 16. At T_1, a new analog commutator input is switched "on," and has until T_3 to complete this switching process. From T_3 to T_4 the analog input drives the voltage-controlled oscillator, and the output frequency is counted. From T_4 to T_6 a new analog commutator input is switched "on." From T_4 to T_5 the

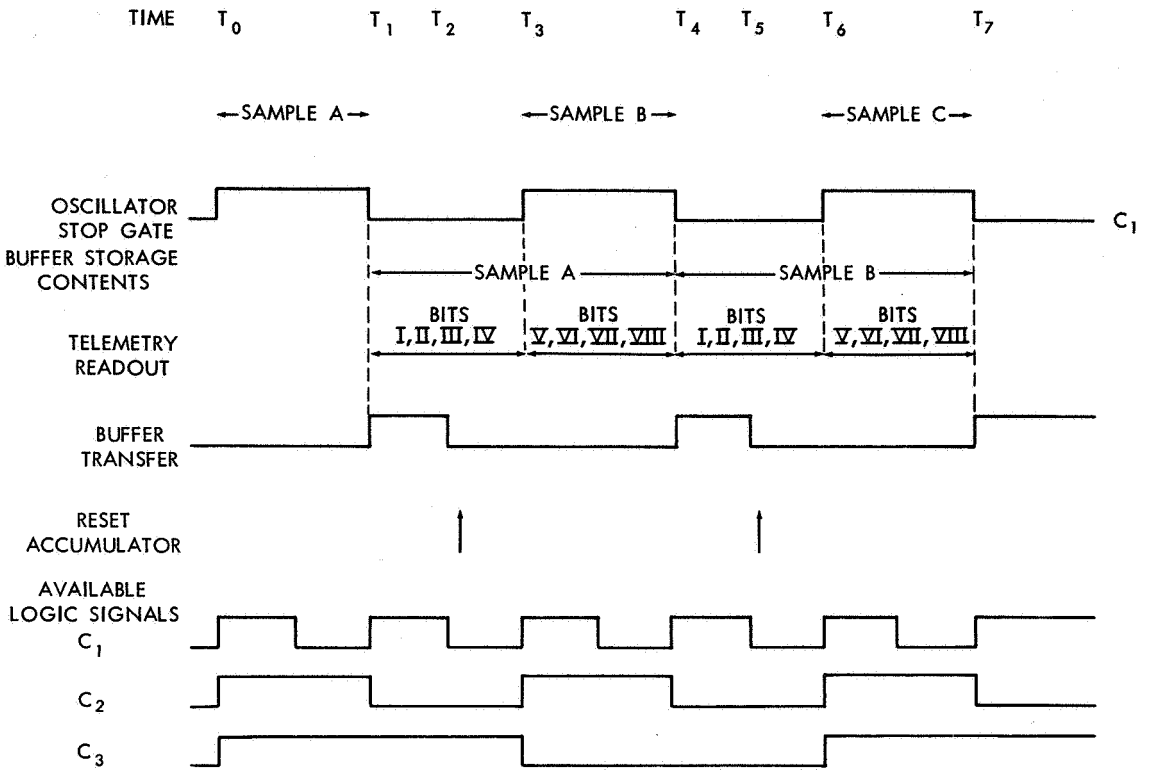

Figure 16—Sequence of events in analog-to-digital conversion.

contents of the accumulator are transferred to a buffer register X. After T_5, the accumulator is reset and soon is ready to count the next sample.

Meanwhile, the least significant bits of sample B are read out into telemetry. From T_6 to T_7 the most significant bits are read into telemetry while sample C is being digitized.

A block diagram of this circuit is shown in Figure 17. The entire accumulator, buffer storage, and readout logic will be about 350 MOSFETS integrated on one chip within a 22 lead round flat pack.

THE ANALOG OSCILLATOR SYSTEM PERFORMANCE

The flight quality analog oscillator performance will be presented, along with calibration procedures and testing methods employed. The data shown in Figure 18 demonstrates that the oscillator could be operated and calibrated over a wide range of voltage inputs and frequency outputs. The detailed system performance will be restricted to the circuit to be used in the IMP H, I, and J, but does not imply that only this range of voltage and frequency range of operation is practical.

Test Equipment Stimulation

The test equipment used to check performance of the analog oscillator is composed of several parts. A set of calibration voltages can be fed into the oscillator manually, or through a flight

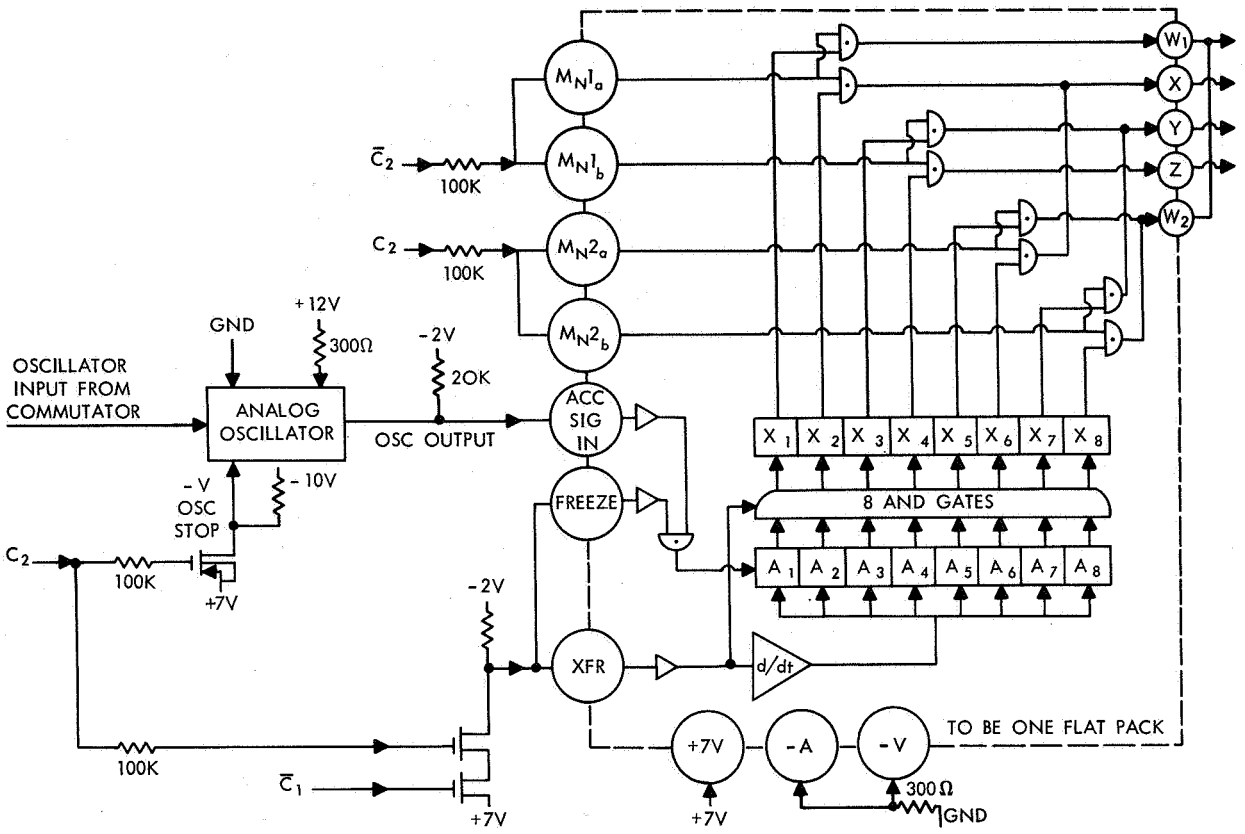

Figure 17—Integrated digital accumulator.

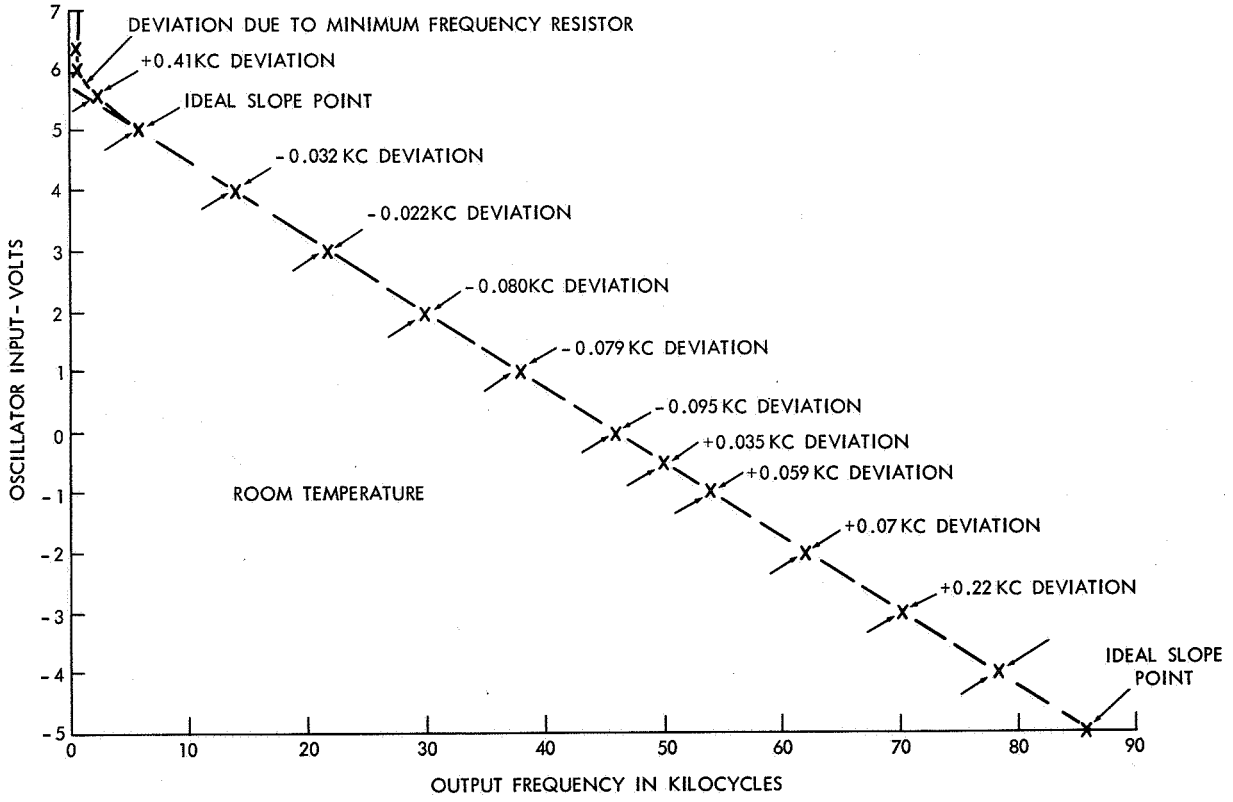

Figure 18—Typical oscillator calibration.

quality MOSFET commutator as previously described. The oscillator can be gated "on" and "off" just as it would be in the flight equipment, with the output counted by a commercial counter and printed at the 3 line per second limit of the printer. The oscillator can be left "on" and the frequency counted to high resolution. Since calibration is needed with greater resolution than flight resolution, the sample time during which the oscillator is gated "on" can be up to 8 times longer than it will be in flight operation. Since the deviation from ideal nominal calibration will be small, only the deviations from nominal will be discussed and plotted.

The analog commutator gates into the analog oscillator under test a series of signals, as shown in Figure 19. The first 8 samples are 1 volt increments over the range, with 1/2 volt checks beyond the normal operating range. Samples 9, 11, and 12 are voltages gated into the oscillator in opposite order from Samples 6, 4, and 2 to check for hysteresis effects of the commutator and oscillator. That is, a large input capacitance or local heating of the input voltage-to-current converting MOSFETS does occur and causes Sample 6 to disagree with Sample 9, Sample 4 to disagree with Sample 11, and Sample 2 to disagree with Sample 12 by about 1/4 of a flight count or about 0.1%.

The commutator Sample 10 is three volts applied through 2 megohms. The slight leakage currents of the MOSFETS, modules, and cables can be detected, and *normally produce* about a ±0.05 kc deviation from the low impedance 3 volt frequency. This represents an 8 millivolt change in voltage or a 2 nanoampere input current to or from the oscillator. This measuring technique is simple but is susceptible to the noise from stray capacitance coupling to the oscillator video output and gating functions.

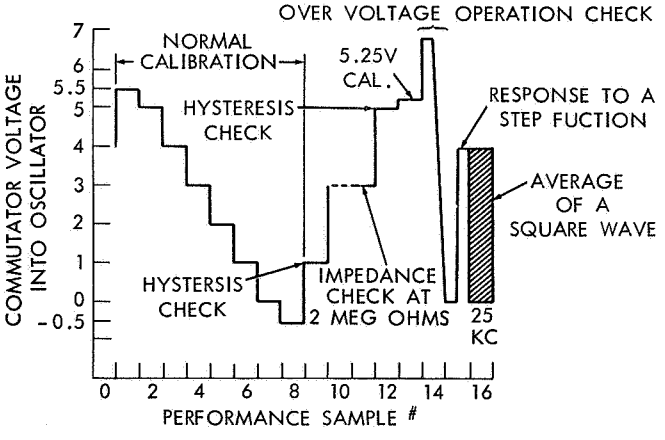

Figure 19—Test equipment commutator output.

The performance Sample 14 applies an abnormally high voltage to the oscillator, and then brings the voltage down quickly. Early in the development program, this test demonstrated a problem and, as a result of this test, the minimum frequency resistor was added to the multivibrator to insure operation even with an instantaneous overvoltage. This test continues to check operation even under such conditions.

The 15th performance sample applies a voltage step function to the oscillator input at the same instant the oscillator is gated "on." Any large capacitance effects through the commutator

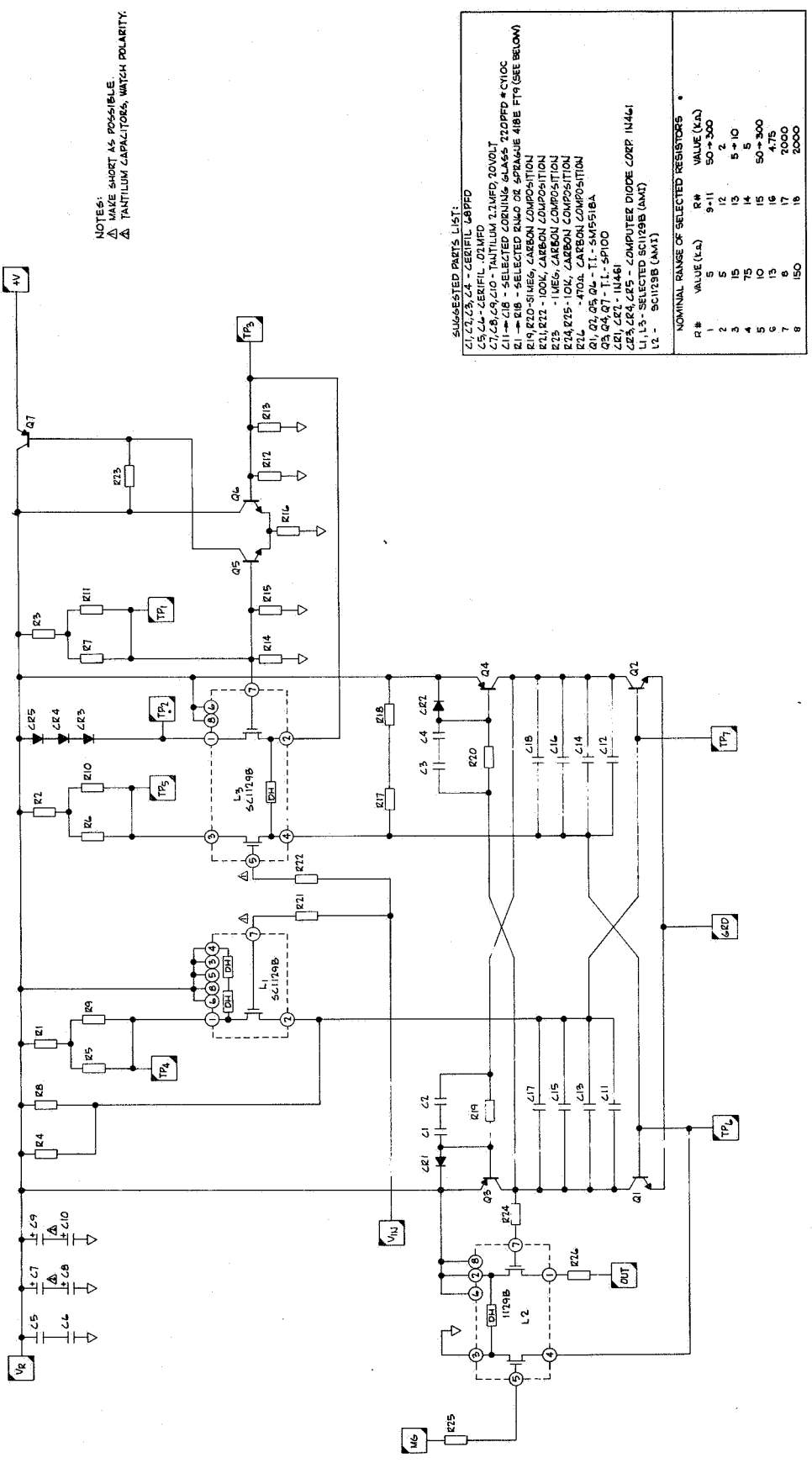

Figure 20—The final analog oscillator circuit.

or at the oscillator input would delay the voltage step and produce a much higher oscillator output count if a problem existed. This specifically checks the phased delays of the 100 k ohm input isolation resistors R_{21} and R_{22} which were added to allow operation to continue if either MOSFET should short due to electrostatic discharge. It is believed this resistance lessens the possibility of such damage and would allow redundant, parallel operation of analog oscillators if desired. The step function is produced by a complimentary transistor inverter to +4 volts, to the matrix gate signal.

The last test applies a 25.6 kilocycle phase-coherent square wave to the oscillator input, between nearly ground and nearly +4 volts. If the oscillator performs a true average of the sample, then the output should be the same as the 2 volt sample. The final oscillator circuit square wave average is less than one count (0.5%) different from the 2 volt calibration. By contrast, such a response from a high impedance transistor emitter follower was found impractical because of the unsymmetrical impedance of such circuits. The MOSFET, however, is symmetric with low capacitance and nearly infinite impedance, thus the MOSFET channel current is modulated proportional to the input voltage, even at a high repetition rate.

Final Analog Oscillator Circuit Calibration

The final oscillator is shown in Figure 20 with several resistor networks in series and parallel to aid calibration. As shown in this diagram, R_7, which is trimmed by R_{11}, allows adjustment of the regulated voltage to make the room temperature frequency at +5 volts nominal. Then R_{10} is increased to trim R_6 if the 3 volt frequency is higher than nominal, or decreased if lower than nominal. Finally R_5, is trimmed with R_9, to adjust the oscillator frequency at ground to the desired frequency. These three adjustments interact, but by successive approximation these three points can be adjusted as close to nominal as desired. The oscillator is then temperature-cycled from -35°C to +85°C. A typical resulting calibration deviation chart is shown in Figure 21.

If the calibration is generally too high in frequency at high temperature and too low in frequency at low temperature, the voltage regulator temperature coefficient can be decreased by increasing R_{12} or trimming resistor R_{13}. A temperature profile of the oscillator is shown in Figure 22 under two different temperature

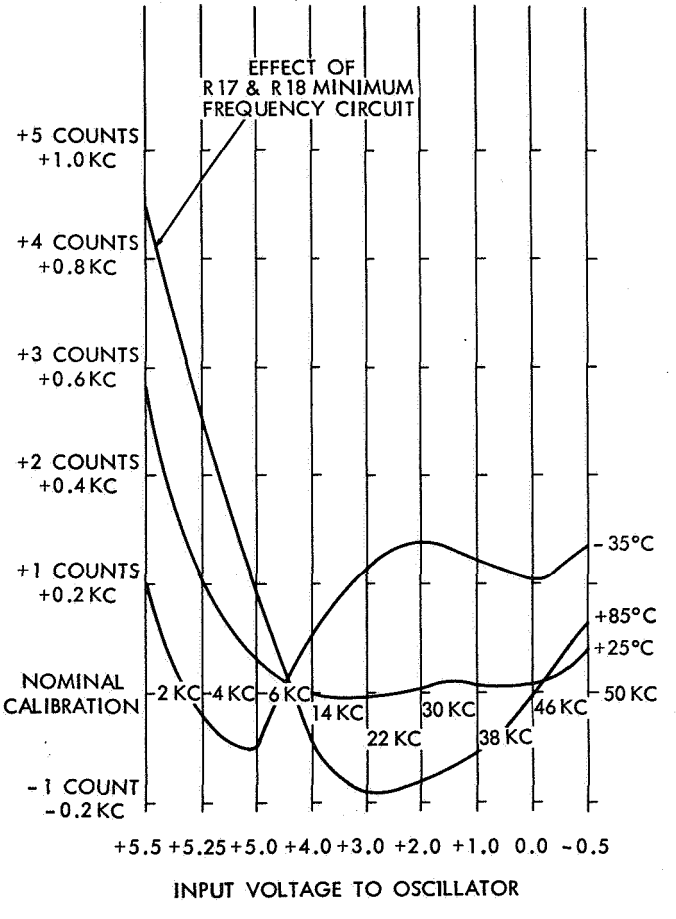

Figure 21—Oscillator calibration deviations from linear ideal.

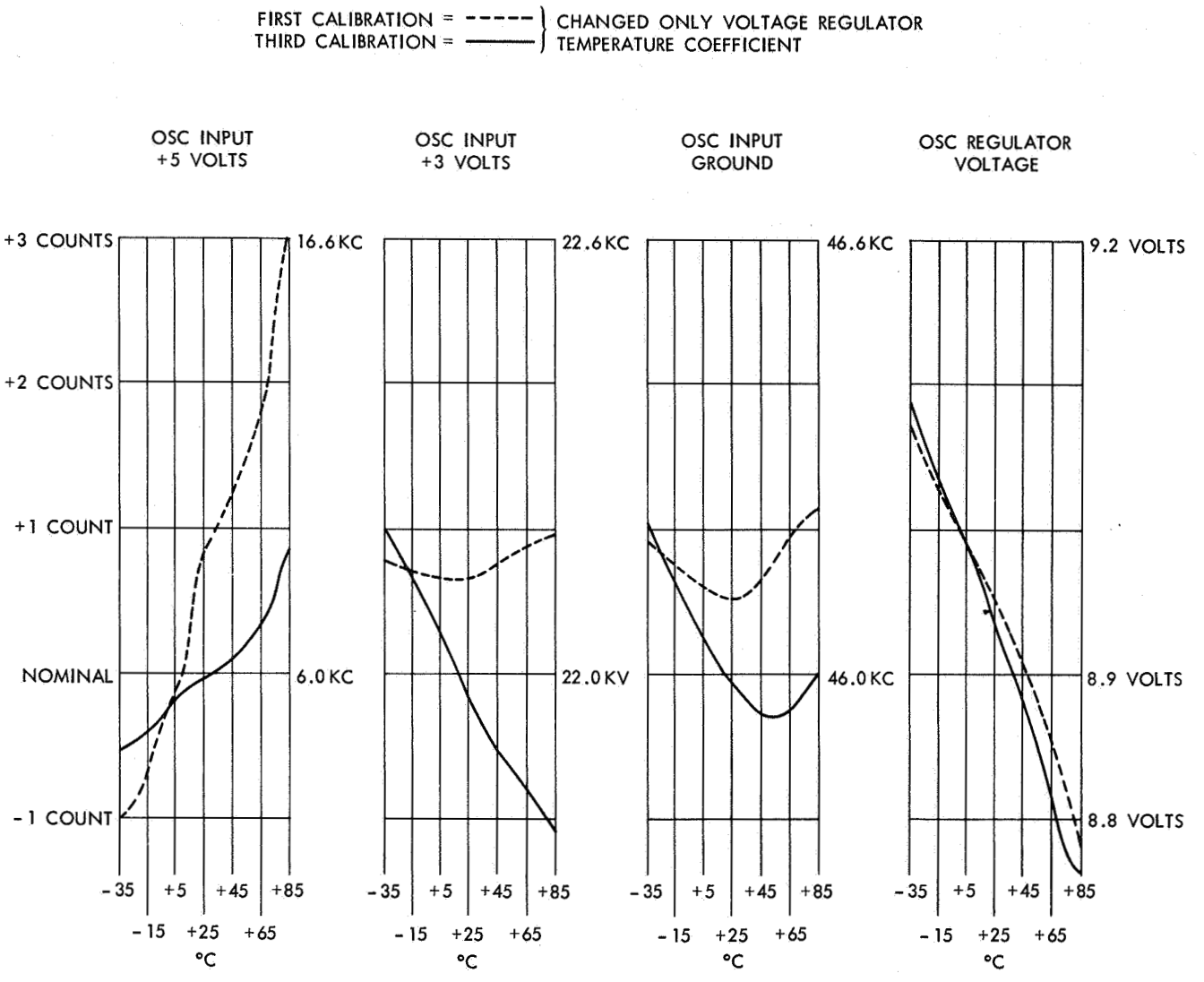

Figure 22—Oscillator temperature profile.

coefficients of the voltage regulator. The positive temperature slope at +5 volts and negative temperature slope at +3 volts are not individually adjustable but are a result of small differences in the temperature coefficient of the MOSFET threshold voltage at different currents. The temperature characteristics with a ground input are also not adjustable, but are affected by the MOSFET in can L_1. Thus a more favorable temperature coefficient MOSFET can be selected for the oscillator. These temperature effects are small for our application. Because the characteristics of the MOSFETS, resistors, and capacitors are so similar, consistency between oscillators is quite easy to obtain to within ±1 count over the -35° to +85° temperature range. The resulting temperature coefficients are within the tolerances needed for this application.

Long Term Stability

The long term stability is another important characteristic of the oscillator which must be verified. Each work day, the room temperature calibration is taken, then the oscillators are

cooled for 3 hours at -35°C. Calibrations are taken and the oscillators are then heated to +85°C. Calibrations are then taken after 3 hours hot. At night the oscillators are normally left with ground input voltage, but occasionally they are left with +5 volts input. A typical result is shown in Figure 23,

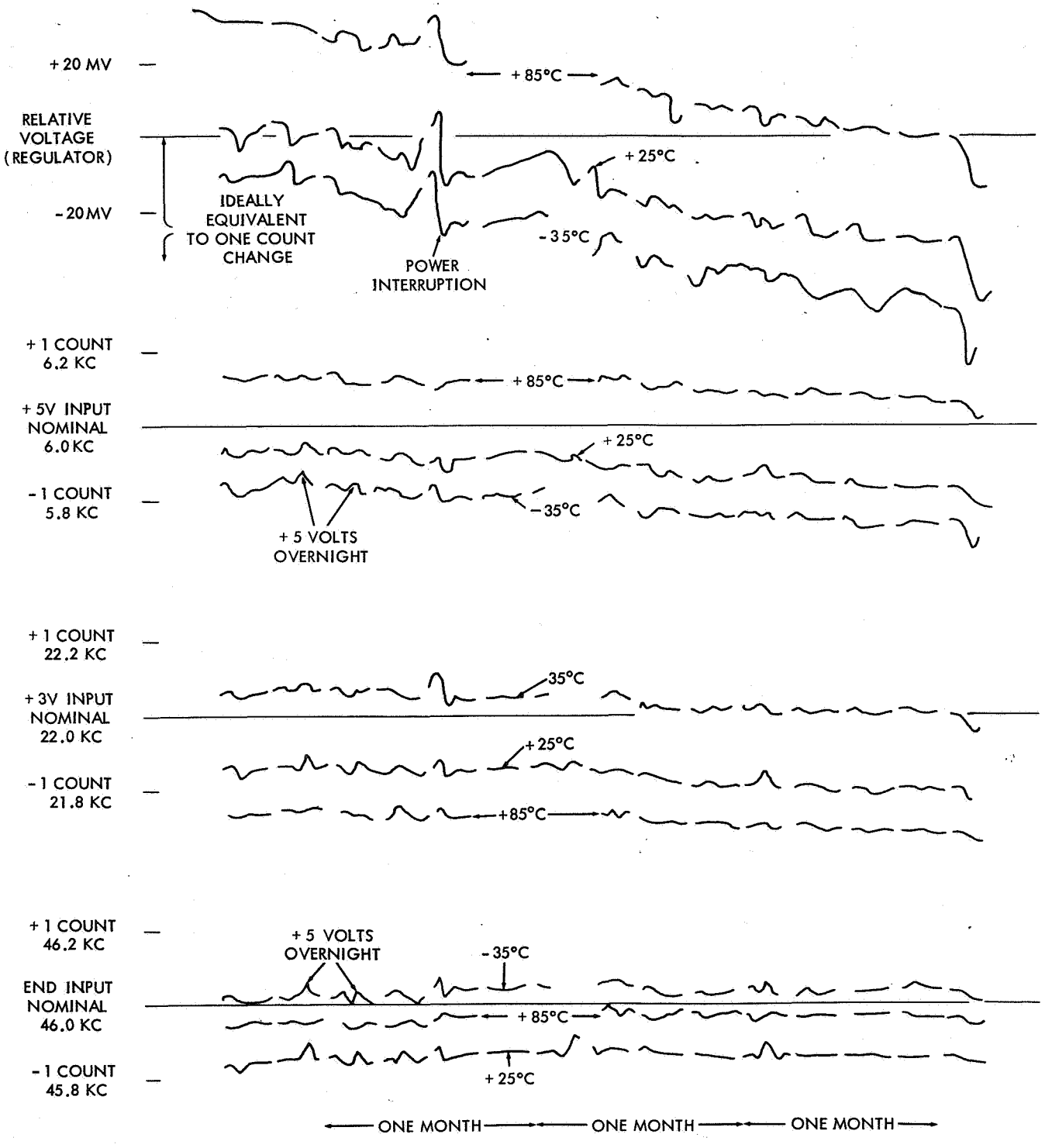

Figure 23—Typical long term stability.

covering a period of over 3 months with about 65 temperature cyclings. The day-to-day repeatability normally appears to be within 1/5 of a count or 0.1% which can be due to a ±2.5 millivolt variation in input voltage. Long term stability appears to be a function of two effects. One multivibrator was operated with fixed resistors in place of the MOSFETS and experienced a 0.048 kc steady increase in frequency over a three month period. This represents 1/4 count increase after about 65 temperature cycles in three months. The regulated voltage slightly increases in some oscillators, and decreases in others. This probably reflects a change in threshold voltage of the MOSFETS within both the regulator and oscillator. If the decrease in MOSFET threshold voltage as shown in Figure 23 had not been compensated for by the decrease in regulator voltage, a 2 count increase in the +5 volt calibration should have occurred. But because the regulator slightly overcompensates for the decrease, the frequency drops almost half-a-count at the 5 volt calibration. However, the long term increase in multivibrator rate causes more of an effect at the ground calibration, increasing the calibration about 1/5 count. The MOSFET voltage change affects the ground end less because such a change is a much smaller percentage of the total frequency determining current.

The effect of leaving the oscillator at +5 volts instead of the customary ground input overnight affects some oscillators more than that shown in Figure 23. The entire calibration will be as much as 1 count or 0.2 kilocycles higher than normal. The speed with which the calibration returns to normal is temperature dependent. At -35°C the calibration is still high by 1/2 count after 4 hours. But at +85°C the calibration returns in a few minutes. This has been found to be due to a change in the MOSFET threshold, and could be some charge migration effect. This effect is not expected to cause any great problem because the analog commutator will not be gating the same voltage into the oscillator for extremely long periods of time, and the hysteresis test shows the problem is less over short sample periods.

Figure 23 shows the long-term stability at the extremes of temperature, with no noticeable variation in temperature coefficient with time. These tests are much more severe both in amount and frequency of temperature cycling than are ever expected in flight. The oscillator appears quite stable even under fast changes in temperature although this is not important in our application.

The characteristics soon after power turn-on are important and are tested by automatically commutating the calibration voltages as soon as power is applied, and comparing them with the calibration five minutes later. Typically, the frequency drops 4 counts from the previous long term calibration, and approaches that value exponentially, and is about 2 counts lower than normal after 5 minutes.

These tests indicate that the largest instability will be at the +5 volt calibration, because of the small differences between the regulator and input MOSFET threshold voltages. Since one of the MOSFETS in the voltage-to-current converter affects the +5 volt frequency calibration much more than the other one, the regulator MOSFET is put in the same can with that one, to minimize temperature and radiation gradients.

The effect from changing the input supply voltage to the regulator is less than 0.1 counts over a range from +10 to +13 volts.

Power Dissipation

The power consumed by the various parts of the oscillator is shown in Figure 24. The regulator consumes the major portion of the power because the load is so small on the regulator. The total current is monitored during testing to insure proper power dissipation.

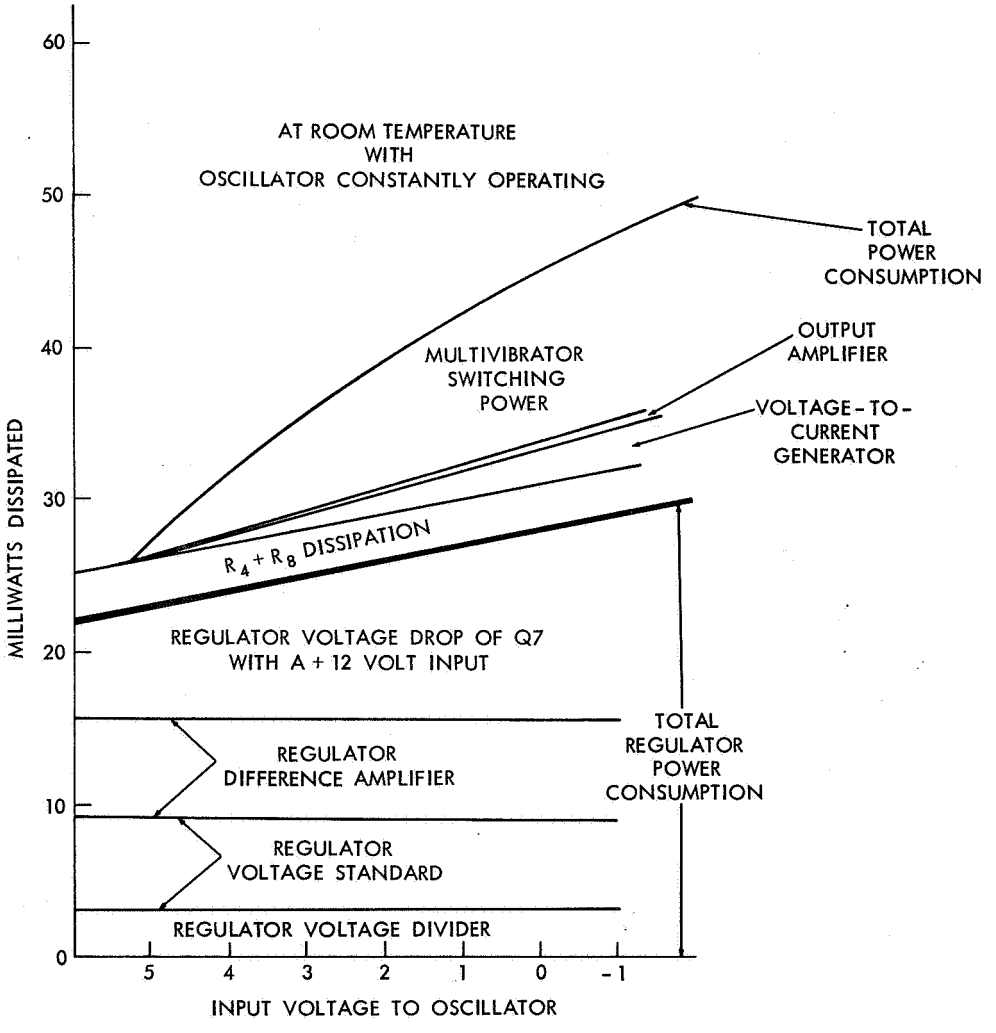

Figure 24—Power consumption breakdown.

Mechanical Layout

The oscillator is calibrated in breadboard form, then the components are assembled in welded modules which are laid out to minimize capacitive coupling between the high speed switching circuits and the high impedance circuits. The change in calibration is about one count due to the reduced stray capacitance. The final stage involves potting the module in ECCO FOAM except for

the trimming resistors. After a month's burn-in, final calibration adjustments are made before final potting of the calibration resistors.

CONCLUSIONS

The analog-to-digital conversion system described utilizes the high impedance input and the easily integrated properties of the MOSFET to achieve a compact, reliable system of superior performance under extreme temperature conditions, with the ability to average a noisy input sample almost perfectly. The saving in cans over previously employed systems is about a factor of three, as shown in Figure 25, and about 40 resistors are saved by being integrated within a chip. The system represents a significant saving in space and weight over those previously employed at about the same power levels.

The magnetic core oscillator previously employed is somewhat more stable but requires considerably more time in which to take an analog sample, and can easily "underflow" the accumulator.

The potential applications for this analog-to-digital conversion system appears quite broad, and may find use where ultra-high input-impedance and microminiaturization are important. The extremely broad range of frequency and voltage over which these concepts could be extended may allow measurements to be made which were impractical previously.

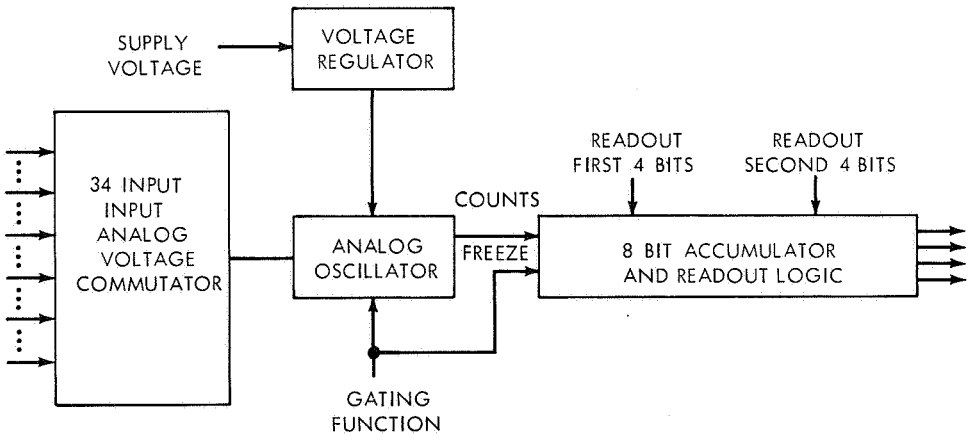

EQUIVALENT SYSTEMS	COMMUTATOR CANS	REGULATOR CANS	OSCILLATOR CANS	ACCUMULATOR CANS	TOTAL CANS
IMP D&E	40	3	13*	21	74
FUTURE IMP'S	22	3	7	2	24

* PLUS MAGNETIC CORE

Figure 25—Savings in cans by more highly integrated MOSFET technology.

ACKNOWLEDGMENTS

The development of this system involved a learning process over a two year period. I wish to acknowledge the excellent job performed by Kenneth Rehmann in the time-consuming developmental testing phase of this work. The final design testing and calibration of twenty flight quality analog oscillators is being performed by Carl Dickson. The excellent uniform linearity and temperature characteristics were obtained by Mr. Dickson through the patient selection of the calibration resistors by successive approximations. I wish to thank him for his perseverence and help in gathering the data which made this report possible.

REFERENCES

1. Bobb, H. S., and Farina, Donald E., "The MOST, A Revolution in Electronic Systems," Second ed., General Mico-Electronics Inc., 1965.

2. De Atley, E. R., ed., "MOS Monolithic Systems: A Revolution in Microelectronics," Philco Corporation, 1966.

3. Lokerson, Donald C., "Implementation of the AIMP D and E Telemetry Encoding System Employing MOSFETS," Goddard Space Flight Center X-711-66-340, 1966.

4. Pound, Alan E., "Application Note AN-01 MOS Low Power Logic," American Micro-Systems, Inc., 1967.

Addendum

Reference 6 has been published in issue of the Atmospheric Sciences, Vol. 24, No. 1, January 1967, pp. 70-79.

Errata

Page 8, Between right hand side of Eq. 10 should be multiplied by a factor of 1/2.

Page 8, First line after Eq. 12: Omit "half".

Figure 6. Same as figure 5, for wall direction in period 1 vs. wall direction in period 3.

Figure 39, line 1: for "0", read " θ ".

Figure 44, line 3 of caption, should read:

"Min. $\beta < 60^{\circ}$; (2) diffuse assumption, with β ; (1) empirical pattern used"

Figure 46, at $\phi = 55^{\circ}$S, read " ϵ_2 " for " ϵ_1 "

Errata

Page 11, second paragraph, fifth sentence should read: "Figure 38 shows the results of these calculations, giving the reflection coefficient and the reflected filtered flux as a function of solar zenith angle. The reflected flux decreases monotonically with solar zenith angle, as a consequence of the cos ζ decrease of the incoming energy per unit horizontal area."

Figure 23, page 39, and figure 32, page 48 should have double-headed arrows along the line $\alpha = 0^\circ$, as follows:

Figure 23

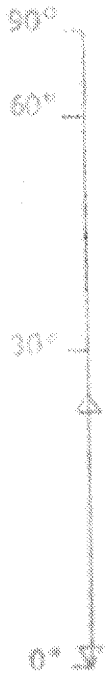

Figure 32

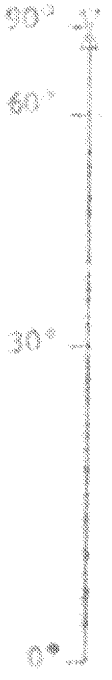

Figures 40, 41, and 42, pages 56, 57, and 58 respectively, should have solid and dashed lines along the θ axis, as follows:

Figure 40

Figure 41

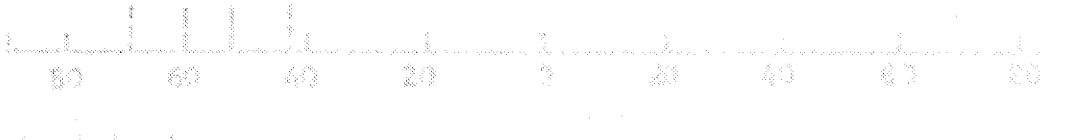

Figure 42